Int. J. Electrochem. Sci., 4 **(2009)** 1452 - 1468

International Journal of ELECTROCHEMICAL SCIENCE
www.electrochemsci.org

Corrosion Behaviour of 6061 Al - 15vol. Pct. SiC Composite and its Base Alloy in a Mixture of 1:1 Hydrochloric and Sulphuric Acid Medium

Geetha Mable Pinto[1], *Jagannath Nayak*[2], *A Nityananda Shetty*[1,*]

[1] Department of Chemistry, National Institute of Technology Karnataka, Surathkal, Srinivasnagar, Karnataka – 575 025.
[2] Department of Metallurgical and Materials Engineering, National Institute of Technology Karnataka, Surathkal, Srinivasnagar, Karnataka – 575 025.
[*]E-mail: nityashreya@gmail.com

Received: 20 September 2009 / *Accepted:* 15 October 2009 / *Published:* 11 November 2009

Silicon carbide particulate - reinforced aluminum (SiCp-Al) composites possess a unique combination of high specific strength, high elastic modulus, good wear resistance and good thermal stability than the corresponding non-reinforced matrix alloy systems. These composites are potential structural material for aerospace and automotive applications. The corrosion characteristics of 6061 Al/SiCp composite and the base alloy were experimentally assessed. The corrosion test was carried out at different temperatures in 1:1 mixture of hydrochloric acid and sulphuric acid at a concentration range of 0.01 to 1N for each of the acid, as corrosion media using Tafel extrapolation technique and Electrochemical impedance spectroscopy (EIS). The results obtained from Tafel extrapolation technique and Electrochemical impedance spectroscopy were in good agreement. The results showed an increase in the corrosion rate with increases in temperature as well as the increase in the concentration of the corrosion media. The thermodynamic parameters like energy of activation were calculated using Arrhenius theory equation and, enthalpy of activation and entropy of activation were calculated using transition state theory equation.

Keywords: Corrosion, Aluminium - silicon carbide composite, Sulphuric acid

1. INTRODUCTION

Aluminium matrix composites (AMCs) have received considerable attention for military, automobile and aerospace applications because of their low density, high strength and high stiffness [1-6]. Further, the addition of ceramic reinforcements (SiC) has raised the performance limits of the Al (6061) alloys [7]. It is known that aluminum matrix composites exhibited better resistance to

mechanical wear than their base alloy and hence they have high specific strength for numerous weight sensitive applications [8, 9]. One of the main disadvantages in the use of metal matrix composite is the influence of reinforcement on corrosion rate. This is particularly important in aluminum alloy based composites, where a protective oxide film imparts corrosion resistance. The addition of a reinforcing phase could lead to discontinuities in the film, thereby increasing the number of sites where corrosion can be initiated and making the composites more susceptible for corrosion [10]. Due to the wide applications of such composites, they frequently come in contact with acid during cleaning, pickling, descaling, etc. Hence studying their corrosion behavior in acid medium is of prime importance. Though, a significant amount of efforts have been spent to understand the corrosion behavior of these composites, the results are not matching since the corrosion resistance of these composites vary with processing techniques, type of reinforcements and particulate size of the reinforcements. Studies on the corrosion behavior of 6061Al-SiC composites in hydrochloric acid medium and controlling the corrosion by using inhibitors have been reported [11, 12]. Hydrochloric and sulphuric acid solutions are used for pickling, chemical and electrochemical etching and in many chemical process industries wherein aluminum composites are used. The study of corrosion behavior of both the base alloy and the composites in 1:1 mixture of hydrochloric acid and sulphuric acid solutions of different concentration and the comparison of their corrosion rates is particularly useful in the field where metal matrix composite is exposed to the corrosion environment containing hydrochloric acid and sulphuric acid.

2. EXPERIMENTAL PART

The experiments were performed with specimens of 6061Al-15 vol.pct. SiC composite and its base alloy in extruded rod form (extrusion ratio 30:1). The composition of 6061 Aluminium base alloy is given in Table 1. Reinforced SiC (average particle size is about 25 micron) has 99.8 percent purity. Test coupons of 1.1 cm and 1.0 cm diameter of the composite and base alloy, respectively, were prepared from the extruded rod and metallographically mounted up to 20 mm height by using cold setting resin. The exposed flat surface of the mounted part was polished with SiC papers to 4/0 grit level and later disc polished using levigated alumina, degreased with acetone and washed with double distilled water and dried.

Table 1. The composition of the base metal Al 6061 alloy.

Element	Cu	Si	Mg	Cr	Al
Composition (Wt.%)	0.25	0.6	1.0	0.25	Balance

AR grade sulphuric acid and hydrochloric acid (Merck) and distilled water were used to prepare 0.01N to 1N acid solutions for all experiments.

Electrochemical measurements were carried out using an electrochemical work station, Autolab 30. For electrochemical measurement, the arrangement used was conventional three electrode Pyrex glass cell with platinum counter electrode and saturated calomel electrode as reference electrode. A water thermostat was used to maintain the required constant temperature.

Finely polished Al-SiC composite specimen and its base alloy with 0.95 cm^2 and 0.79 cm^2 surface areas, respectively, were exposed to corrosion medium of different concentrations of 1:1 mixture of hydrochloric and sulphuric acid (0.01 N to 1 N) at different temperatures of 303 K to 323 K. The potentiodynamic current-potential curves were recorded by polarizing the specimen to -250 mV cathodically and +250 mV anodically with respect to open circuit potential (OCP) at a scan rate of 0.01 V/s.

Electrochemical impedance spectroscopy (EIS) measurements were carried out using a small amplitude ac signal of 10 mV over a frequency range of 100 kHz-0.01 Hz. The experiments were repeated at least three times.

3. RESULTS AND DISCUSSION

3.1. Polarization measurements

Fig. 1 represent the potentiodynamic polarization curves of 6061Al base alloy and its composite with SiC in 1:1 mixture of hydrochloric and sulphuric acid solutions of different concentrations at 50°C. The corrosion current densities (i_{corr}) obtained by the Tafel extrapolation technique increases with increase in concentration of the acid mixture in the solution for both the samples.

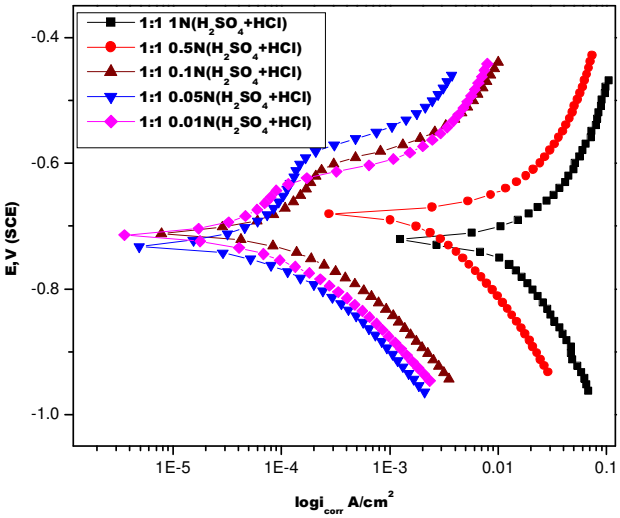

Figure 1a. Tafel plots of base alloy at different concentrations of 1:1 acid mixture solution at 50°C

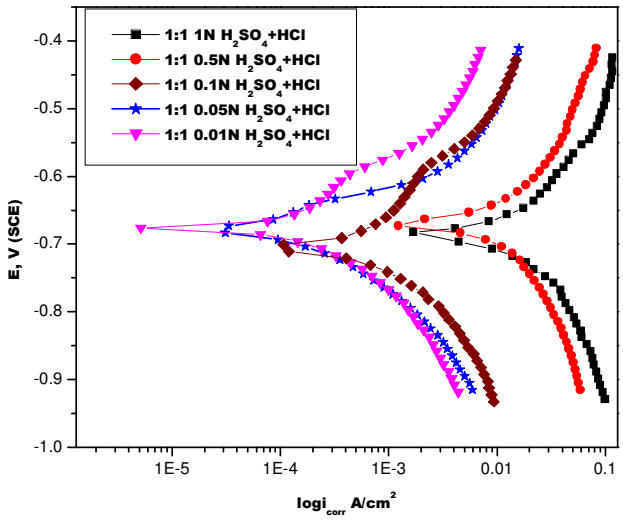

Figure 1b. Tafel plots of composite at different concentrations of 1:1 acid mixture solution at 50°C

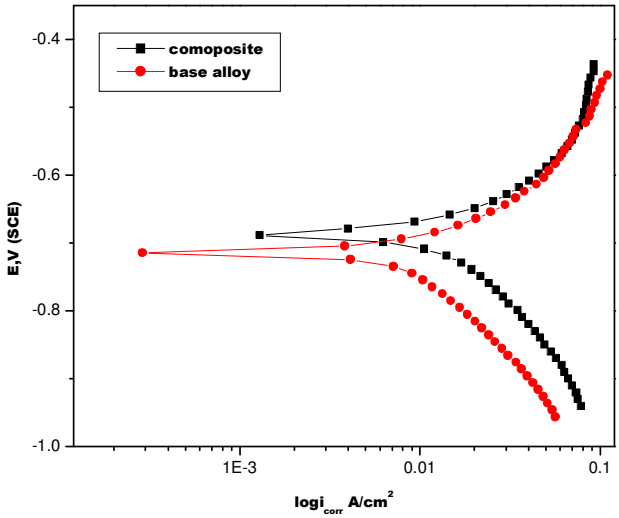

Figure 2. Tafel extrapolation plots for base alloy and the composite in 1N 1:1 acid mixture solution at 35°C

Fig. 2 represents the Tafel extrapolations for the base alloy and the composite in 1N acid mixture solution at 35°C. The corrosion current density values indicate that the composite undergoes more corrosion than the base alloy.

3.2. Electrochemical impedance spectroscopy measurements

Nyquist plots of the base alloy and the composite in mixture of acid solution of different concentrations at 50°C are given in Fig. 3. As can be seen from the Fig. 3, the impedance diagrams show semicircles, indicating that the corrosion process is mainly charge transfer controlled [10,13].

The general shape of the curve is similar for all individual samples of the base alloy and composite, with large capacitive loop at high frequencies (HF) and an inductive loop at low frequencies (LF). Similar impedance plots have been reported in literature for the corrosion of pure aluminum and Al alloys in various electrolytes such as sodium sulphate [14, 15,16], sulphuric acid [15,17] acetic acid [17], sodium chloride [16, 18] and hydrochloric acid [19-26].

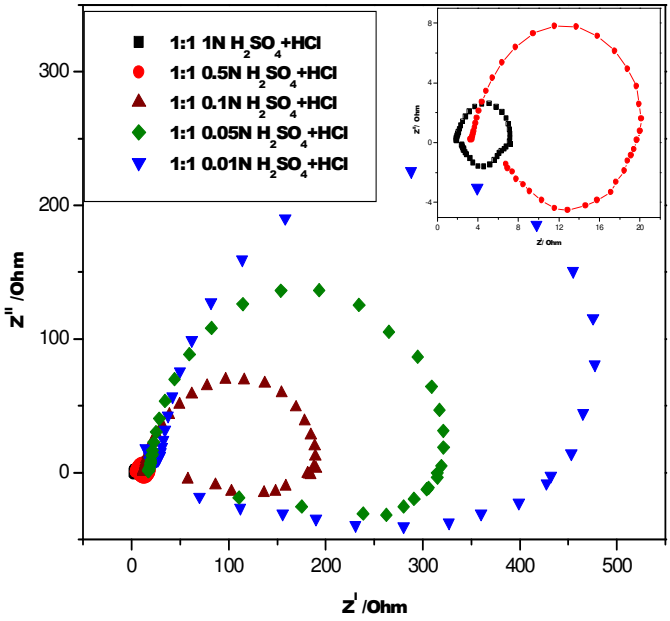

Figure 3a. Nyquist plots of base alloy at different concentrations of 1:1 acid mixture solution at 50°C.

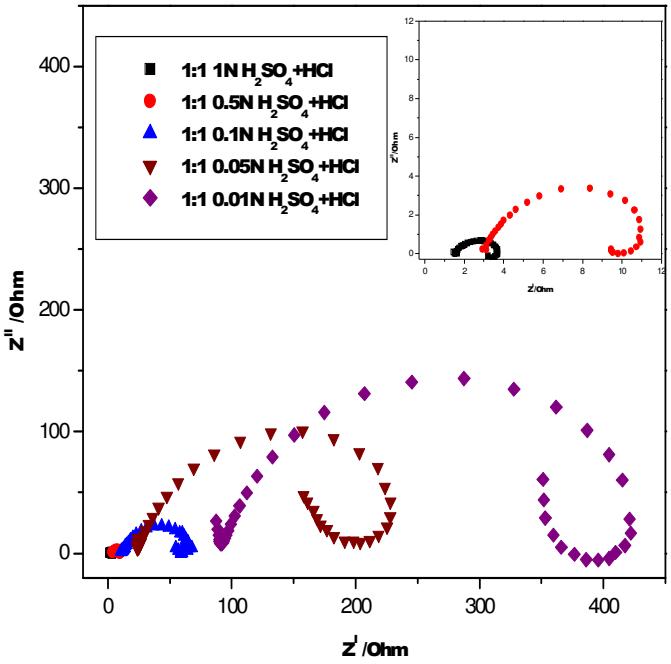

Figure 3b. Nyquist plots of composite at different concentrations of 1:1 acid mixture solution at 50°C.

The HF capacitive loop is attributed to the presence of a protective oxide film covering the surface of the composite. According to Brett [20, 22], the capacitive loop is corresponding to the interfacial reactions, particularly, the reaction of aluminium oxidation at the metal/oxide/electrolyte interface. The process includes the formation of Al^{+} ions at the metal/oxide interface, and their migration through the oxide/solution interface where they are oxidized to Al^{3+}. At the oxide/solution interface, OH^{-} or O^{2-} ions are also formed. The fact that all the three processes are represented by only one loop could be attributed either to the overlapping of the loops of processes, or to the assumption that one process dominates and, therefore, excludes the other processes [17]. The other explanation offered to the high frequency capacitive loop is the oxide film itself. This was supported by a linear relationship between the inverse of the capacitance and the potential found by Bessone et. al [27] and Wit et. al [28].

The origin of the inductive loop has often been attributed to surface or bulk relaxation of species in the oxide layer [18]. The LF inductive loop may be related to the relaxation process obtained by adsorption and incorporation of chloride and sulphate ions on and into the oxide film [14].

An equivalent circuit of five elements depicted in Fig.4 and Fig 5 was used to simulate the measured impedance data as shown in Fig. 4b and Fig. 5b. It consists of a constant phase element (CPE) Q in parallel with the parallel resistors R_t (charge transfer resistance) and R_L (inductance resistance) and the later is in series with the inductor L. When an inductive loop is present, the polarization resistance Rp can be calculated from,

$$Rp = \frac{R_L \ X \ R_t}{R_L + R_t} \quad \text{..... (1)}$$

It was observed that the value of CPE decreases while the value of Rp increases with increasing concentration of acid mixture.

The measured value of polarization resistance increases while the CPE value decreases with increasing concentration of the acid mixture, indicating that the rate of corrosion increases with increase in concentration of acid mixture solution in both the cases of base alloy and composite. This is in agreement with the results obtained from potentiodynamic polarization data.

It is seen from the impedance spectra that the frequency range over which the samples display capacitive behavior is narrower in the case of composites than in the case of base alloy. The narrower frequency range observed indicates that the natural oxide layer formed is less protective in the case of composites. The addition of SiC as a reinforcing phase could have led to discontinuities in the protective film, thereby increasing the number of sites where corrosion can be initiated and causing higher corrosion on the composite [10]. Also, the reinforcement of silicon carbide is highly cathodic to the matrix and causes the galvanic effect at the interfaces between the matrix and the reinforcement. These results are consistent with the potentiodynamic polarization data obtained.

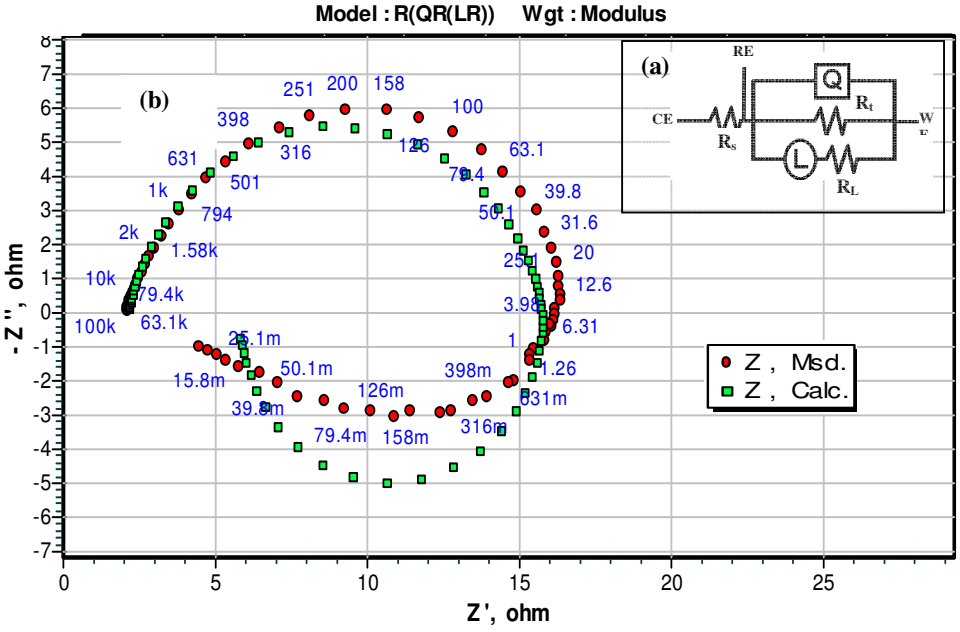

Figure 4. The equivalent circuit model used to fit the experimental data of the base alloy in 1N 1:1 acid mixture solution.

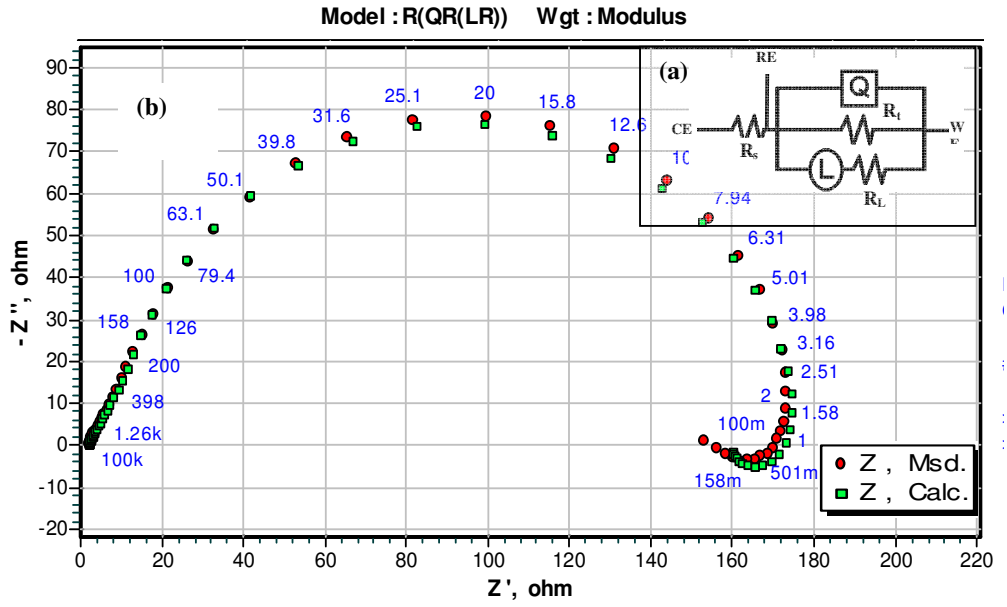

Figure 5. The equivalent circuit model used to fit the experimental data of the composite in 0.05N 1:1 acid mixture solution.

3.3. Effect of temperature

The effect of temperature on the corrosion rate of the base alloy and the composite was studied by measuring the corrosion rate at different temperature between 30-50°C. Fig. 6 represents the potentiodynamic polarization curves at different temperatures for the base alloy and the composite in 1N acid mixture solution. Fig. 7 represents Nyquist plots for the same. Fig 6 shows the variation of corrosion rate with temperature for the base alloy and the composite in acid mixture solution of varying concentrations. From the Fig. 8, it is clear that the corrosion rate increases with temperature for both the base alloy and the composite in the entire concentration range of acid mixture studied. The observation could be related to the fact that, as the temperature increases the oxide passive film becomes thin, porous and less protective as a result of dissolution of the film by the electrolyte [29].

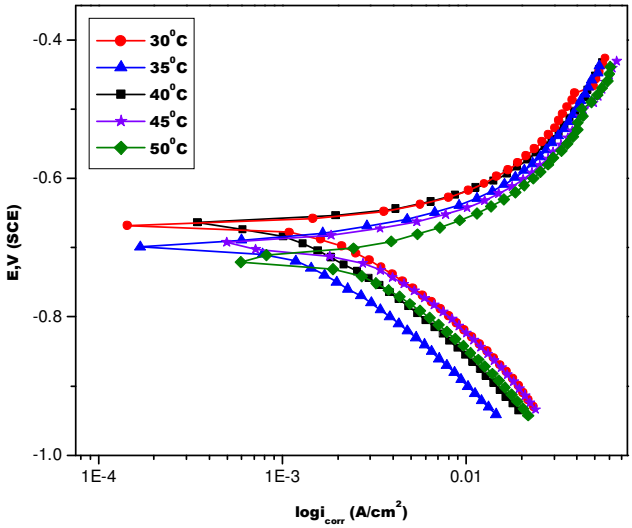

Figure 6a. Tafel plots of base alloy at different temperatures in 0.5N 1:1 acid mixture solution.

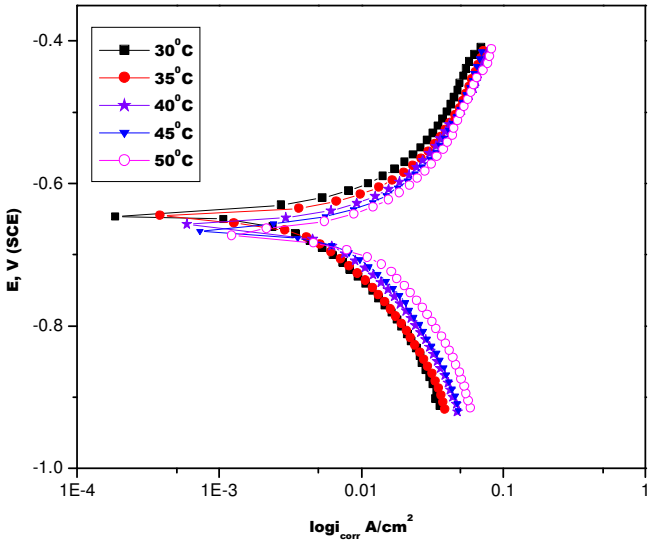

Figure 6b. Tafel plots of composite at different temperatures in 0.5N 1:1 acid mixture solution.

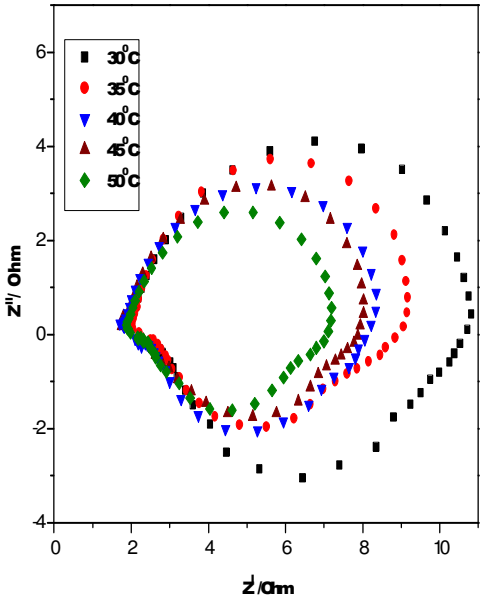

Figure 7a. Nyquist plots of composite at different temperatures in 1N 1:1 acid mixture solution.

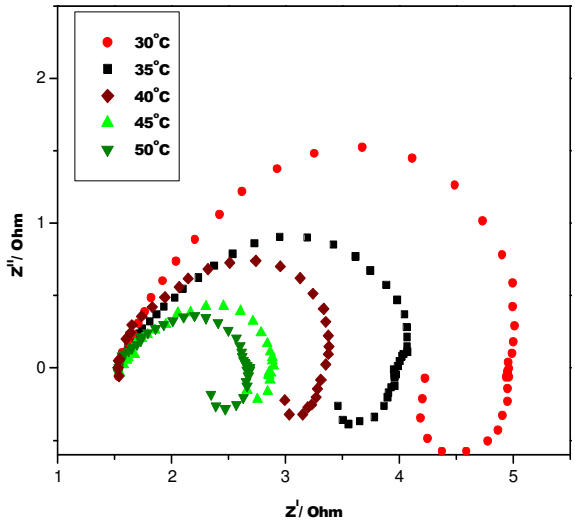

Figure 7b. Nyquist plots of composite at different temperatures in 1N 1:1 acid mixture solution.

The energy of activation of corrosion for the base alloy and the composite were calculated from the Arrhenius plot (lnCR vs 1/T) at all the concentrations of sulphuric acid studied (Fig 9).

Arrhenius equation,

$$C.R = A\, e^{-\frac{Ea}{RT}} \quad \text{.....(2)}$$

where A is constant and R is ideal gas constant.

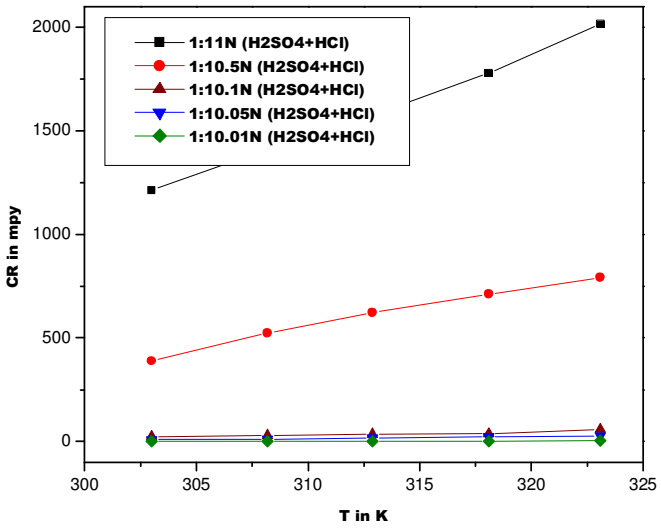

Figure 8a. Effect of temperature on the corrosion rate of the base alloy.

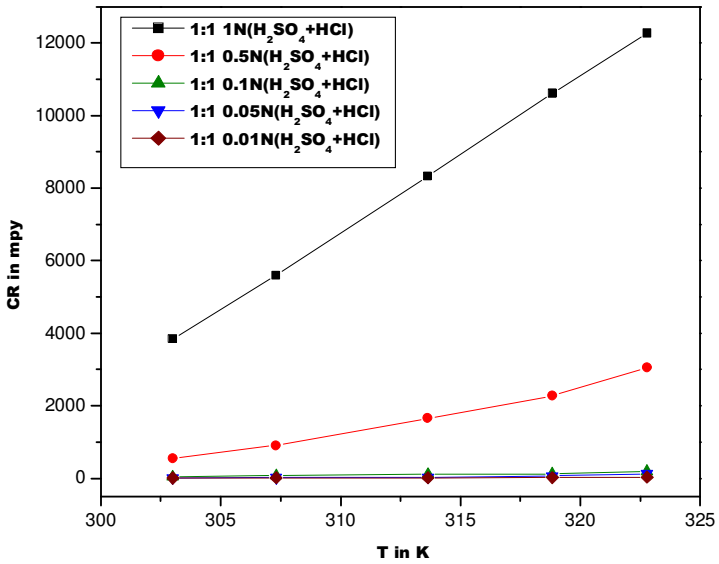

Figure 8b. Effect of temperature on the corrosion rate of the composite.

Enthalpy of activation (ΔH) and entropy of activation (ΔS) were calculated from the transition state theory equation,

$$C.R = \frac{RT}{Nh} e^{\frac{\Delta S}{R}} e^{-\frac{\Delta H}{RT}} \quad .....(3)$$

where h is plank's constant, N is Avogadro's number.

A plot of ln(CR/T) vs 1/T gives straight line with slope = -ΔH/R and intercept = ln(R/Nh) +ΔS/R.

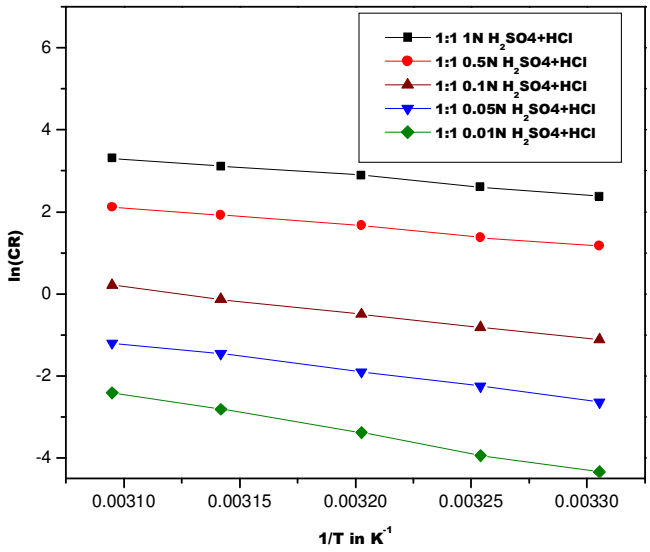

Figure 9a. Arrhenius plots for the base alloy.

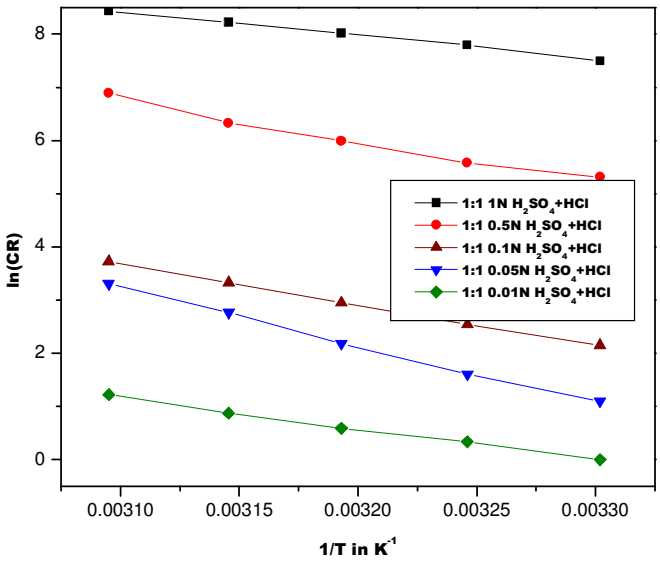

Figure 9b. Arrhenius plots for the composite.

Fig. 10 gives the plot of ln(CR/T) vs 1/T for the base alloy and composite in various concentrations of acid mixture. The values of energies of activation, enthalpy of activation and entropy of activation are listed in table 2.

Table 2. Activation energy, Enthalpy of activation and Entropy of activation for the composite and the base alloy

Conc of H_2SO_4 (N)	Ea (kJ/mol)		ΔH (kJ/mol)		-ΔS (J/K/mol)	
	Composite	Base alloy	Composite	Base alloy	Composite	Base alloy
0.01	49.56	57.88	48.34	55.36	137.19	191.23
0.05	46.33	54.89	44.67	52.65	121.56	182.25
0.1	41.59	49.90	40.11	47.36	109.25	171.02
0.5	40.19	46.93	38.64	44.16	103.01	146.58
1	38.77	41.57	36.12	43.68	90.96	118.65

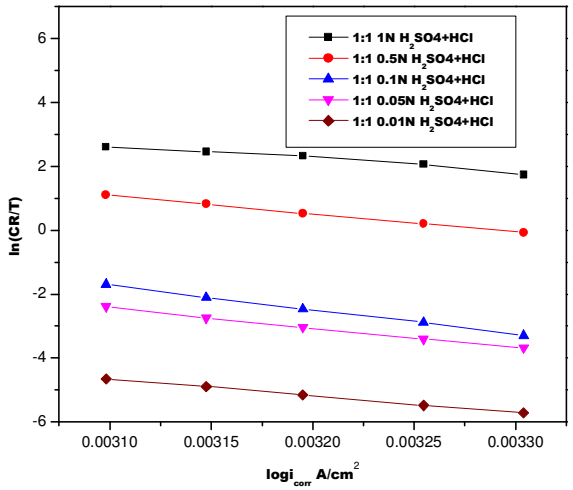

Figure 10a. ln(corrosion rate/T) vs 1/T for base alloy at different concentrations.

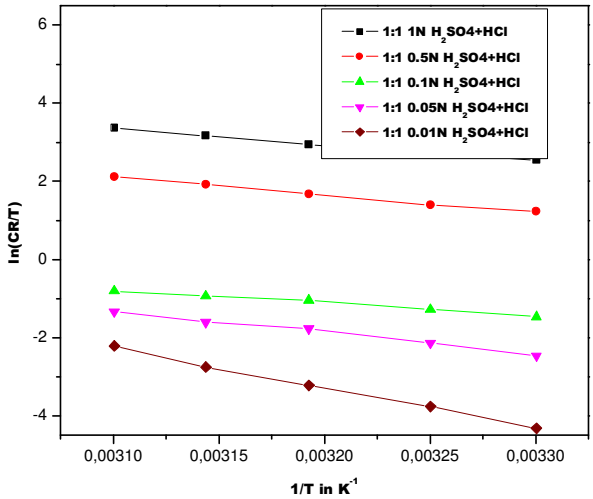

Figure 10b. ln(corrosion rate/T) vs 1/T for composite at different concentrations.

Data presented in table 2, infer that activation energy for the base alloy is higher than that for the composite in all concentration of acid mixture, confirming the suggestion that the corrosion resistance of the base alloy is higher than that of the composite.

The electrochemical parameters i_{corr} , anodic Tafel slope b_a, and cathodic Tafel slope b_c , that is associated with the polarization measurements at different concentrations and temperatures of the acid mixture for both the base alloy and the composite are summarized in table 3 and table 4 respectively.

The impedance parameters R_s, R_p, CPE and corrosion rate that is associated with the polarization measurement at different concentrations and temperatures of the acid mixture for both the base alloy and the composite are summarized in table 5 and table 6, respectively.

Table 3. Results of Tafel polarization studies, for the base alloy.

Condition		**Tafel extrapolation**				
Medium	**Temp**	**Icor (x 10 $^{-5}$A)**	**Rp (ohm)**	**b_c (V/dec)**	**b_a (V/dec)**	**CR (mpy)**
0.01N H_2SO_4+HCl	303	0.4	4782	0.064	0.05	2
	308	0.5	3536	0.062	0.05	3
	313	0.6	3001	0.062	0.06	4
	318	0.7	2028	0.048	0.07	5
	323	0.9	856	0.045	0.04	11
0.05N H_2SO_4+HCl	303	0.9	1838	0.096	0.05	5
	308	1.4	1436	0.035	0.03	7
	313	2.8	1101	0.154	0.07	15
	318	3.5	977	0.157	0.08	19
	323	4.6	498	0.158	0.09	22
0.1N H_2SO_4+HCl	303	2.6	1028	0.095	0.060	15
	308	3.4	904	0.100	0.059	19
	313	4.2	835	0.111	0.059	21
	318	5.3	514	0.112	0.061	29
	323	7.4	281	0.126	0.064	35
0.5N H_2SO_4+HCl	303	51.8	27	0.023	0.07	283
	308	68.7	20	0.058	0.026	376
	313	72.9	16	0.044	0.118	400
	318	102.4	15	0.030	0.079	561
	323	179.5	11	0.071	0.146	983
1N H_2SO_4+HCl	303	315.4	8	0.051	0.084	1438
	308	443.8	7	0.074	0.098	1550
	313	586.1	6.5	0.107	0.101	1588
	318	676.9	6.1	0.112	0.112	1730
	323	789.3	5.1	0.114	0.116	2024

Table 4. Results of Tafel polarization studies for the composite.

Condition		Tafel extrapolation				
Medium	**Temp**	**Icor (x 10 $^{-5}$A)**	**Rp (ohm)**	**b_c (V/dec)**	**b_a (V/dec)**	**CR (mpy)**
0.01N H_2SO_4+HCl	303	0.73	898.0	0.128	0.106	4
	308	0.90	762.0	0.130	0.110	6
	313	3.59	640.0	0.132	0.112	15
	318	4.60	410.0	0.134	0.114	22
	323	6.90	110.0	0.135	0.115	29
0.05N H_2SO_4+HCl	303	2.58	656.8	0.098	0.117	31
	308	3.57	460.0	0.105	0.118	34
	313	4.42	300.9	0.109	0.125	47
	318	6.48	182.7	0.114	0.128	64
	323	8.33	143.5	0.120	0.130	98
0.1N H_2SO_4+HCl	303	10.45	204.2	0.076	0.134	70
	308	13.54	155.7	0.081	0.133	99
	313	16.64	100.0	0.090	0.140	110
	318	24.24	88.4	0.096	0.146	124
	323	27.47	66.8	0.100	0.150	144
0.5N H_2SO_4+HCl	303	232.0	16.1	0.057	0.102	1035
	308	261.5	10.1	0.059	0.119	1165
	313	376.0	4.28	0.079	0.141	1677
	318	487.6	3.37	0.098	0.148	2177
	323	599.5	2.97	0.118	0.121	2675
1N H_2SO_4+HCl	303	910.2	2.38	0.101	0.152	3858
	308	939.2	1.99	0.112	0.176	4173
	313	975.1	1.78	0.123	0.112	4330
	318	1253.0	1.52	0.131	0.119	7559
	323	1562.0	1.10	0.136	0.124	8858

Table 5. Results of electrochemical impedance studies for the base alloy.

Medium	**Temp**	**Rs (ohm)**	**Rp (ohm)**	**CPE (µF)**	**Corrosion rate (mpy)**
0.01N H_2SO_4+HCl	303	61.7	4918	4	2
	308	60.3	3637	5	3
	313	59.1	3031	7	4
	318	58.6	2030	8	5
	323	55.3	897	10	12
0.05N H_2SO_4+HCl	303	32.0	1954	5	6
	308	28.7	1482	6	7

	313	30.5	1107	8	10
	318	27.6	979	10	11
	323	29.9	500	13	22
	303	19.1	1051	7	10
	308	10.9	938	10	12
0.1N H_2SO_4+HCl	313	13.1	862	13	13
	318	14.0	530	20	19
	323	13.6	236	25	46
	303	3.7	28	18	389
	308	3.6	21	23	524
0.5N H_2SO_4+HCl	313	3.2	17	27	638
	318	2.9	15	31	724
	323	2.8	12	33	771
	303	2.2	8.9	28	1213
	308	2.1	7.2	32	1508
1N H_2SO_4+HCl	313	1.8	6.8	38	1575
	318	1.7	6.2	41	1728
	323	1.6	5.4	46	2016

Table 6. Results of electrochemical impedance studies for the composite.

Medium	**Temp**	**Rs (ohm)**	**Rp (ohm)**	**CPE (µF)**	**Corrosion rate(mpy)**
	303	58.4	920	15	11
	308	57.3	637	26	17
0.01N H_2SO_4+HCl	313	55.6	530	32	19
	318	53.7	420	46	24
	323	50.1	340	58	32
	303	27.3	728	24	15
	308	21.6	442	48	25
0.05N H_2SO_4+HCl	313	22.7	349	64	31
	318	23.2	159	88	68
	323	24.6	83	101	129
	303	12.3	266	65	41
	308	11.9	140	137	77
0.1N H_2SO_4+HCl	313	16.8	101	184	108
	318	10.8	92	240	118
	323	11.2	57	288	193
	303	4.0	19.8	94	543
	308	3.8	11.9	150	905
0.5N H_2SO_4+HCl	313	3.0	6.5	237	1654
	318	3.1	5.6	286	1945
	323	2.8	3.5	314	3047

	303	1.5	2.61	152	4134
	308	1.4	2.16	348	4961
1N	313	1.6	1.24	556	8661
H_2SO_4+HCl	318	1.5	1.01	623	10826
	323	1.7	0.91	823	11890

4. CONCLUSIONS

A systematic study of the corrosion behavior of 6061 Aluminium alloy and its composite Al-15 vol. Pct. SiC composite in different concentrations of 1:1 mixture of hydrochloric acid and sulphuric acid at different temperatures by electrochemical methods lead to the following conclusions.

- The potentiodynamic polarization and impedance studies of the corrosion behavior of 6061 aluminium alloy and its composite Al-15 vol. Pct. SiC in 1:1 mixture of acid solutions showed that the corrosion resistance of the base alloy is greater than that of the composite.
- The corrosion rate for both the base alloy and composite increases with increase in the concentration of acid mixture.
- The corrosion rate for the base alloy and the composite increases with temperature.

References

1. T. H. Sanders Jr., E. A. Starke Jr., *Proceedings of the Fifth International Conference on Al–Lithium alloys, Materials & Composites*, Engineering Publications Ltd., Birmingham, UK, 1989, pp. 1–40.
2. C. Monticelli, F. Zucchi, G. Brunoro, G. Trabanelli, *J. Appl. Electrochem*., 27 (1997) 325.
3. A. Pardo, M. C. Merino, S. Merino, F. Viejo, M. Carboneras, R. Arrabal, *Corros. Sci,*. 47 (2005) 1750.
4. C. E. Da Costa, F. Velasco, J. M toralba, *Rev. Metal. Madrid,* 36 (2000) 179.
5. P. K. Rohatgi, *JOM.*, 43 (1991) 10.
6. A. Pardo, M. C. Merino, S. Merino, M. D. Lopez, F. Viejo, M. Carboneras, *Mater.Corros*., 54 (2003) 311.
7. C. J. Peel, R. Moreton, P. J. Gregson, E. P. Hunt, *Proceedings of the XIII, International Conference on Society of Advanced Material and Process Engineering*, SAMPE, Covina, CA, 1991, pp. 189.
8. M. Hutchings, S. Wilson, A. T. Alpas, T.W.Clyne (ed.), *Comprehensive Composite Materials*, Vol.3, Elsevier Science Ltd., UK, 2000, pp. 501-505.
9. D. M Aylor, *Corrosion of Metal Matrix Composites, Metals Hand Book*, Vol.13, Ninth Edition, ASM, 1987, pp. 859.
10. A. J. Trowsdate, B. Noble, S .J. Haris, I.S. R. Gibbins, G. E. Thomson, G. C. Wood, *Corros. Sci*., 38 (1996) 177.
11. Suma A Rao, Padmalatha, J. Nayak and A. N. Shetty. *J. Met. and Mat. Sci*., 47 (2005) 51-57.
12. Suma A Rao, Padmalatha, J. Nayak and A. N. Shetty. *Trans. of the SEAST,* 41 (2006) 01-04.
13. G. Trabanelli, C. Montecelli, V. Grassi, A. Frignani, *J. Cem. Concr., Res*. 35 (2005) 1804.

14. S. Sayed, Abdel Rehim, Hamdi H. Hassan, A. Mohammed, Amin, *Applied Surf. Sci*., 187 (2002) 279.
15. J. H. Wit and H. J. W. Lenderink, *Electrochim. Acta,* 41 (1996) 1111.
16. J. B. Bessone, D. R. Salinas, C. Mayer, M. Ebert and W. J. Lorenz, *Electrochim. Acta,* 37 (1992) 2283.
17. H. J. W. Lenderink, M. V. D. Linden, J. H. W. Dewit, *Electrochem. Acta*, 38 (1993) 1989.
18. S. E. Frers, M. M. Stefenel, C. Mayer and Chierchie, *J. Appl. Electrochem*., 20 (1990) 996.
19. M. Metikos-Hukovic, R. Babic and Z. Grubac, *J. Appl. Electrochem*., 28 (1998) 433.
20. C. M. A. Brett, *J. Appl. Electrochem*., 20 (1990) 1000.
21. E. J. Lee and S. I. Pyun, *Corros. Sci*., 37 (1995) 157.
22. C. M. A. Brett, *Corros. Sci*., 33 (1992) 203.
23. K. F. Khaled, M. M. Al-Qahtani, *Mater. Chem. Phys*., 113 (2009) 150-158.
24. Ehteram A. Noor, *Mater. Chem. Phys*., 114 (2009) 533-541.
25. A. Aytac, U. Ozmen, M. Kabasakaloglu, *Mater. Chem. Phys*., 89 (2005) 176-181.
26. M. Metikos-Hukovic, R. Babic and Z. Grubac, *J. Appl. Electrochem*., 32 (2002) 35.
27. J. B. Bessone, C. Mayer, K. Jutner, W. J. Lorenz, *Electrochim Acta,* 28 (1983) 171.
28. J. H. Wit, C. Wijenberg, C. Crevecoeur, *J. Electrochem. Soc.,* 126 (1979) 779.
29. R.T. Foley, T. H. Nguyen, *J. Electrochem. Soc*., 129 (1982) 464.